

Journal of Materials Chemistry B

Accepted Manuscript



This is an *Accepted Manuscript*, which has been through the Royal Society of Chemistry peer review process and has been accepted for publication.

Accepted Manuscripts are published online shortly after acceptance, before technical editing, formatting and proof reading. Using this free service, authors can make their results available to the community, in citable form, before we publish the edited article. We will replace this *Accepted Manuscript* with the edited and formatted *Advance Article* as soon as it is available.

You can find more information about *Accepted Manuscripts* in the [Information for Authors](#).

Please note that technical editing may introduce minor changes to the text and/or graphics, which may alter content. The journal's standard [Terms & Conditions](#) and the [Ethical guidelines](#) still apply. In no event shall the Royal Society of Chemistry be held responsible for any errors or omissions in this *Accepted Manuscript* or any consequences arising from the use of any information it contains.

ARTICLE

Shape Memory Behaviour of HA-g-PDLLA Nanocomposites Prepared via *in-situ* Polymerization

Cite this: DOI: 10.1039/x0xx00000x

Ke Du,^{a,b} and Zihua Gan^{a,b*}Received 00th January 2012,
Accepted 00th January 2012

DOI: 10.1039/x0xx00000x

www.rsc.org/

The shape memory property of hydroxyapatite-*graft*-poly(D,L-lactide) (HA-g-PDLLA) nanocomposites was investigated in the present study. The hybrid nanocomposites with various HA proportions (5, 10, 15 and 25wt%) were prepared via *in-situ* grafting polymerization. It is found that nanocomposites exhibit various shape memory (SM) performances with different HA loading. The excellent shape memory properties were performed by HA-g-PDLLA nanocomposites with 15wt% inorganic HA proportions, observed through a well-established four-step SM programming cycle method. However, at low HA loading (including pure PDLLA), the samples experienced a severe relaxation process, which caused a plastic, irreversible deformation of the sample and resulted in the poor SM recovery ratio. Besides, the shape memory behaviours of HA25-g-PDLLA nanocomposites and HA25/PDLLA blends were compared. Due to the serious relaxation process caused by the weak interaction forces of hydrogen bonding between HA and PDLLA, the HA25/PDLLA blends performed much worse shape recovery ability than the HA25-g-PDLLA nanocomposite.

1. Introduction

Shape memory polymers (SMPs) are one class of smart materials that has attracted increasingly attentions, especially in the last two decades, due to its stimuli-responsive properties.¹⁻³ Shape memory materials can transform their shape as a response of certain external stimulus,⁴ such as light,⁵ pH,⁶ irradiation,⁷ electricity,⁸ as well as temperature.^{3, 9-11} Among these materials, thermal induced SMPs have got more concerns because of their intrinsic superiorities such as low cost, excellent processibility, and good recovery ability. The mechanism of thermal induced SMPs has been introduced in many literatures.¹²⁻¹⁴ In a typical description, the materials are deformed when it is heated above its transition temperature (T_{trans}). The imposed stress is remained when the designed strain reached a certain value and unloaded when the environmental temperature dropped below T_{trans} . Shape recovery occurs as long as the SMPs are reheated above the T_{trans} value, which can be either a glass transition temperature (T_g) or a melting temperature (T_m) of the polymer.¹⁵ SMPs have wide applications in different fields on the basis of such 'memorize' properties. The applications cover various areas including textile,¹⁶ packaging,^{12,17} and especially medical industries.¹⁸ With regard to medical industries, it is predicable that the SMPs would have inspiring prospects in minimally

invasive surgery applications. Own to the stimuli-responsive properties, the SMPs can be implanted into human body with a small size in "temporary shape" state, and then allowed to recovery their original shape *in vivo* under certain thermal stimuli. Currently studies focus on surgical and implantable devices for therapeutics and diagnosis like self-expanding stents,^{19,20} intelligent sutures,²¹ thrombectomy devices,²² and active catheters.^{23,24} Moreover, intelligent drug delivery matrices have shown attractive and potential applications involving self-anchoring subcutaneous implants and slowly deploying low-force devices for local drug release to organs enclosed by the material.¹ Up to now, metallic alloys are commonly used shape memory materials in practical application. However, bioresorbable SMPs are promising candidates for replacement of metallic alloys because, as a contrast, they do not need additional operation for removal after implantation.²⁵ Consequently, these multifunctional polymers with combined shape-memory property and bioabsorbability will play a key role as medical devices. Synthetic poly(ϵ -caprolactone) (PCL), polylactide (PLA), polyglycolide (PGA) and the copolymers of PLA and PGA (PLGA) are typical bioresorbable polymers, which are widely used in the fabrication of scaffolds for tissue engineering. One of the major drawbacks is the lack of intrinsic bioactivity,

which results in the deficiency in inducing positively regenerative response from bone cells when implanted.²⁶ Consequently, the incorporation of bioactive ceramics (e.g. hydroxyapatite) into polymer matrixes is an available method to solve this problem. Hydroxyapatite (HA) shows appropriate osteoconductivity and biocompatibility owing to the chemical and structural similarity to the mineral phase of native bone. It has been reported that the interactions of osteogenic cells with HA leads to the improved ability of bone bonding and regeneration.²⁷ In addition, the incorporation of HA which was functionalized as reinforced filler could improve the mechanical properties of neat PLA and thus make it adequate for high-load-bearing application in biomedical field. However, generally, one major difficulty in fabricating this hybrid composites is the homogeneously dispersion of inorganic particles in polymer matrixes. To effectively avoid the aggregation of inorganic particles, *in-situ* grafting polymerization method is employed to prepare the hybrid nanocomposites. The purpose of this approach is to graft organic polymer chains to the hydroxyl groups of HA particles through covalent bonding.²⁸

Zhou reported shape memory behaviours of PDLA/HA composites prepared by physically blending method.^{29, 30} The hydrogen bonding, which exists between PDLA chains and HA particles, was responsible for the higher shape recovery, compared with pristine PDLA. The hydrogen bond serves as physical cross-linking points and endows the nanocomposites with shape memory properties. Normally, given to the mechanism of shape memory property, bonding force between inorganic fillers and polymer matrixes should be preferentially considered. The materials should possess some degree of chemical crosslinking to form a “memorable” network or contain a finite fraction of hard regions as physical crosslinks. Taking such concerns into consideration, the HA-g-PDLA nanocomposites, which have chemical bond connection between HA and PDLA chains, possess stronger interaction force between soft regions and hard regions compared with the hydrogen bond interaction in the case of PDLA/HA blends. However, attempt to investigate the shape memory property of HA-g-PDLA nanocomposites synthesized via *in-situ* polymerization and to compare with the physical HA/PDLA blends has not been well studied before.

Herein, we introduce a novel approach to prepare SMPs. The HA-g-PDLA nanocomposites with different HA fractions were prepared via *in-situ* grafting polymerizations for the study of shape memory property. We emphasized the effect of chemical bonding between inorganic particles and organic polymers on the SM behaviours of nanocomposites. Based on the results, the stable nano-level dispersion of grafted HA nanoparticles in PDLA matrix is critical in its shape memory properties compared with HA/PDLA blends which were prepared by solution blending. To the best of our knowledge, the investigation of interfacial affinity of HA and PDLA and its influence on the shape memory property of HA-g-PDLA nanocomposites has not yet been reported.

2. Experimental Section

2.1 Materials.

D,L-lactide (Purac Co.) was purified by recrystallization from dry ethyl acetate and then subsequently dried in a vacuum oven for 72h prior to use. Toluene was purified by distillation in the presence of metallic sodium and benzophenone. Stannous octoate ($\text{Sn}(\text{Oct})_2$) solution in toluene (Aldrich) was diluted in dried toluene and stored under argon atmosphere. Hydroxyapatite nanoparticles (nHA) was purchased from Aldrich and dried in vacuum oven at 100°C for 48h before use. The nanoparticles present white colour and spherical shape, with a molecular formula $[\text{Ca}_5(\text{OH})(\text{PO}_4)_3]_x$ and molecular weight of 502.31g/mol. The product number from the manufacturer is 677418. The HA utilized in the present study is synthetic degree, with a phase purity higher than 97%. As shown in the product specification, the particles size $\leq 200\text{nm}$ and the specific surface area $\geq 9.4 \text{ m}^2/\text{g}$. All the other reagents were used as received.

2.2 *In-situ* grafting polymerization of HA-g-PDLA nanocomposites

The grafting polymerization of PDLA to HA nanoparticles was carried out in reaction tube under vacuum conditions. The typical polymerization procedures were as follows: nHA (2.5g) and DLLA (7.5g) were added in the dried reaction tube under argon atmosphere. Then, freshly dried toluene (30ml) was added into the reaction tube. The solution of $\text{Sn}(\text{Oct})_2$ in dry toluene with the molar ratio of $[\text{DLLA}]/[\text{Sn}(\text{Oct})_2]$ as 500 was added to initiate the reaction. The polymerizations was carried out at 120°C for 48h under argon atmosphere. After then, the reaction tube was quenched to room temperature, and the products were purified by dissolving in dichloromethane and precipitating in cold methanol twice before use. All the samples prepared via *in-situ* grafting polymerization were noted as HAx-g-PDLA, where x presents the HA percentage content in the nanocomposites.

2.3 Preparation of PDLA/HA nanocomposites blends

To prepare the PDLA/HA blends, a two-step method was utilized for dispersion of the HA nanoparticles in polymer solution. At beginning the HA nanoparticles were dispersed in dichloride methane (CH_2Cl_2) and sonicated at room temperature. Then the PDLA (Mn=80k, PDI=1.4, synthesized in our group) solution in CH_2Cl_2 was added into the HA/ CH_2Cl_2 dispersion, making sure that the HA proportion in PDLA/HA mixture is 25wt%. The final products were precipitated by cold methanol twice before use.

2.4 Preparation of samples for SM study

All the samples were dried in vacuum oven at 80°C for 72h in order to eliminate the residual solvent. Then the nanocomposites were hot-pressed into designed shape (10mm thickness) by using metal moulds. The obtained nanocomposite stripes were then cooled at room temperature and prepared for the further use.

2.5 Analysis and characterization:

The thermal properties of samples were analysed on a Pyris Diamond differential scanning calorimeter (DSC, Perkin

Elmer). All operations were performed under nitrogen purge, and the weight of all the samples varied between 6~7mg. Samples were first melt at 150°C for 5min to eliminate thermal history, and then cooled to -20°C at a rate of 10°C/min, and finally heating to 140°C at a rate of 20°C/min. The thermal gravimetric analysis (TGA) of all samples were performed on a thermo-gravimetric analyzer (Pyris 1, Perkin Elmer) by heating from room temperature to 650°C at a rate of 20°C /min with a nitrogen flow rate of 20ml/min. The morphology of the cross-section of HA-g-PDLLA nanocomposites was observed by field-emission scanning electron microscopy (JEOL JSM-6700F Japan) after coating with gold in vacuum.

2.6 Shape memory (SM) behaviour

The dynamic mechanical measurements of nanocomposite samples were carried out on a dynamic mechanical analyzer (Q800 DMA, TA Instruments) in tensile mode. The analyses were conducted using a preload force of 0.01N, oscillation amplitude of 15µm and a frequency of 1Hz. The shape memory behaviours of all samples were quantitatively evaluated by a four-step procedure. Typically, the strip with 6.5cm in width and 0.13cm in thickness was stretched at T=60°C from 0MPa to 0.2MPa with a rate of 0.02MPa/min. Without releasing the sample from the grips, the deformed sample (i.e., the temporary shape) was fixed by quenching to 0°C at 3°C/min. Then the stress of samples was released to 0MPa at a rate of 0.05MPa/min. After then the SM behavior was performed when heating to 70°C again at a rate of 3°C/min. The macroscopic SM evaluation of pure PDLLA and HA-g-PDLLA nanocomposites was carried out and recorded by a digital camera. All samples with different letter shapes and the same thickness of 0.15cm were deformed at 70°C, stored at -20°C to maintain its temporary shape and recovered its permanent shape at 70°C.

3. Results and Discussion

3.1 Characterization of HA-g-PDLLA nanocomposites:

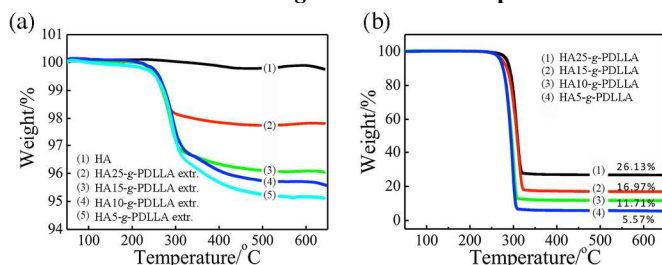


Fig 1. (a) TGA curves for HA, HA25-g-PDLLA, HA15-g-PDLLA, HA10-g-PDLLA and HA5-g-PDLLA extractions. All extractions were thoroughly washed by dichloromethane; (b) TGA curves of as-obtained HA5-g-PDLLA, HA10-g-PDLLA, HA15-g-PDLLA and HA25-g-PDLLA. The number after HA denotes the weight percentage of HA in nanoparticles.

The grafting polymerization of DLLA monomers from the hydroxyl groups of HA and the polymerization mechanism have been reported.^{31,32,33} To confirm whether the grafting polymerization have been successfully performed on the surfaces of the HA nanoparticles, the proportion of free PDLLA

chains initiated by impurities other than the hydroxyl groups on the surface of HA nanoparticles should be extracted from the HA-g-PDLLA composite prior to the next characterization. Dichloromethane was used to extract the soluble part of free PDLLA chains from its composites containing different proportions of HA.

Figure 1a shows the weight loss curves of HA-g-PDLLA nanocomposites after extraction. As listed in Table1, the weight percentage of burning residue was 2.2% and 5.1% for HA25-g-PDLLA and HA5-g-PDLLA, respectively, indicating the decreased initiation efficiency of HA with increasing proportion of HA in the reaction mixture, which is in good accordance with the results reported by Helwig et al.³¹ Figure 1b shows the TGA curves of the as-obtained HA-g-PDLLA nanocomposites with different HA proportions. The weight percentages of the burning residue are 26.13%, 16.97%, 11.71% and 5.57% for HA25-g-PDLLA, HA15-g-PDLLA, HA10-g-PDLLA and HA5-g-PDLLA, respectively. It is obvious that the actual proportion of the HA in the as-obtained nanocomposites were in good accordance with the feed ratio in the reaction mixtures, which reflects that the monomer conversion was relatively high for the *in-situ* grafting polymerizations in the presence of HA nanoparticles, as clearly shown in Table1.

Table 1. Properties of HA-g-PDLLA nanocomposites

Sample	Mn ^a	PDI ^a	Yield %	Grafting ratio ^b %	HA ^b content%	Tg ^c °C
HA25-g-PDLLA	80,000	1.74	99	2.2	26.13	54.0
HA15-g-PDLLA	79,000	1.63	98	3.9	16.97	54.4
HA10-g-PDLLA	72,000	1.81	98	4.4	11.71	53.5
HA5-g-PDLLA	86,000	1.76	97	5.1	5.57	50.9
PDLLA	71,000	1.55	92	-	-	40.1

^a Molecular weight (Mn) and polydispersity index (PDI) determined by GPC;

^b Obtained from TGA results;

^c Glass transition temperature determined by DSC.

3.2 Dispersion of HA nanoparticles in PDLLA matrixes

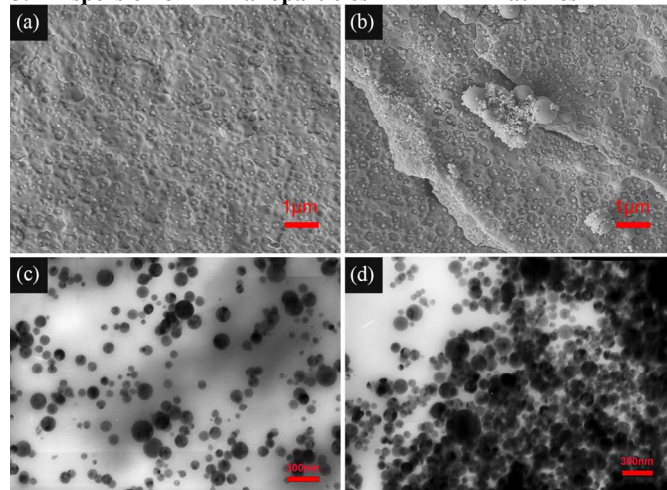


Fig 2. SEM images of cross-section morphologies of (a) HA25-g-PDLLA nanocomposites and (b) HA25/PDLLA blends. (c) & (d) are TEM images of bulk ultra-thin section of nanocomposites and blends, respectively.

The dispersion state of the inorganic fillers in polymer matrixes plays a key role in crystallization, thermal and mechanical properties of hybrid nanocomposites. It has been known that the HA nanoparticles were prone to agglomerate in polymer matrixes or solutions. So in order to investigate whether *in-situ* polymerization method has improved the dispersibility of HA nanoparticles in PDLLA matrixes, an intuitive comparison between the physical blends and the *in-situ* polymerization products by SEM and TEM analysis was carried out.

Figure 2 shows the cross-section morphologies of HA25-g-PDLLA nanocomposites and HA25/PDLLA blends. For nanocomposites, the uniform dispersion of HA nanoparticles was observed in PDLLA matrix, as shown in Fig2a & Fig2c. While in the case of blends (Fig2 b&d), the HA nanoparticles tend to form micro-scaled agglomeration. This phenomenon may be due to the inter-particle Vander Waals interaction and the hydrogen bonding between surface hydroxyl groups.³⁴⁻³⁶

3.3 Thermal and mechanical properties

Figure 3a shows the DSC heating curves of HA-g-PDLLA nanocomposites with different HA proportions. In each DSC curve, the stepwise specific heat increment associated with the glass transition is the only thermal feature observed, which suggested that nanocomposites only single-phased with no evidence of phase separation. The glass transition temperatures (T_g) are listed in Table 1. The results show that in the range from -20°C to 140°C , the investigated nanocomposites exhibit a tendency of possessing a higher T_g with increasing the HA contents in the nanocomposites, which is in agreement with the well-known effect of the filler content on the chain segment movement of the matrixes. However, it should be pointed out that the highest T_g was observed in the case of HA15-g-PDLLA, the value of which is 54.4°C .

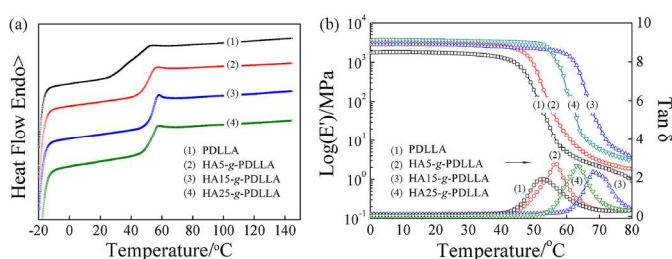


Fig 3. (a) The DSC traces of all tested samples from the second heating rounds; (b) The Plots of tensile storage modulus (E') and $\tan \delta$ (b) against temperature for PDLLA polymer, HA5-g-PDLLA, HA15-g-PDLLA and HA25-g-PDLLA nanocomposites

Dynamic mechanical spectroscopy was also analysed. Figure 3b plots the storage modulus and $\tan \delta$ changes of hybrid nanocomposites with different HA proportions against temperature. For the storage modulus curves, as shown in the temperature range of $T < T_g$, the investigated samples were glassy with a unchanged tensile storage modulus which was only dependence on HA contents. It is known that introducing fillers into the polymer matrix is one of the common methods for increasing elastic modulus of the materials.¹² Our results show a consistent tendency that the storage moduli increase

with increasing proportion of HA component in the nanocomposites. One of the reasons could be attributed to the reinforced interaction force between grafted HA nanoparticles and PDLLA polymer chains in HA-g-PDLLA nanocomposites. Besides, the grafted HA nanoparticles took over some free volume and thus hindered the mobility of polymer chains. The above explanations account for the increment of the elastic modulus of nanocomposites. When the temperature is higher than T_g , the increasing molecular mobility allows for the stored elastic energy to be released as a mechanical restoring force and for the material to recover its permanent original shape.¹² It is reported that the higher elastic modulus in glassy state is better for the shape fixation of SMPs in low temperature.³⁷ Comparisons of our results suggest that the storage modulus loss of HA25-g-PDLLA ($3685 \rightarrow 3.068\text{MPa}$) is more obvious than pure PDLLA ($1749 \rightarrow 0.914\text{MPa}$), which accord with the report that the larger storage modulus loss value is benefited to the shape memory performance.³⁸

In correspondence to the modulus step, the dependence of $\tan \delta$ on temperature was also shown in Figure 3b. Owing to the well-known frequency effect,²⁵ the glassy transition temperature observed through $\tan \delta$ -T curves was not corresponding to the T_g data obtained by DSC analysis. However, $\tan \delta$ -T curves were corresponding with the storage modulus E' and show a general tendency that the T_g values rise with increasing the proportion of HA component and the highest T_g was achieved for the nanocomposites with 15wt% of HA nanoparticles. These results show that the binding effect of the grafted HA nanoparticles to PDLLA chains is more prominent when the HA nanocomposite fraction is in an appropriate range (e.g. 15%).

3.4 Shape memory properties

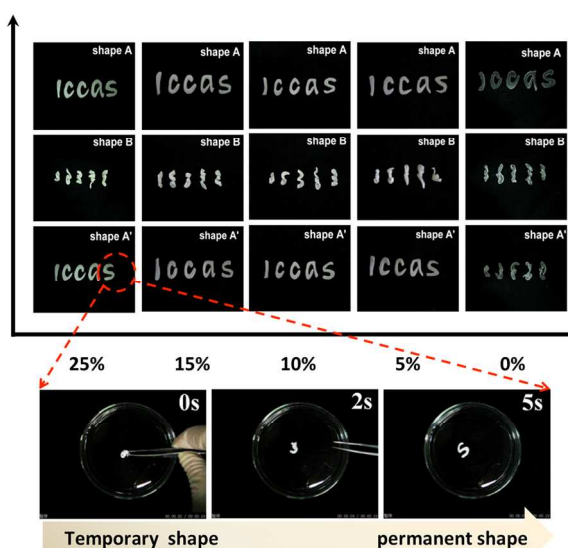


Fig 4. Time series photographs of shape recovery of HA-g-PDLLA nanocomposites with different HA proportions.

The thermal induced shape memory polymers (SMPs) could respond mechanical reaction triggered by the external stimulus.

By controlling environmental temperature, the SMPs possess the ability to memorize a permanent shape that can substantially differ from their initial temporary shape.²¹ Figure 4 shows a visual comparison of shape recovery capacity of HA-g-PDLLA nanocomposites with different HA proportions (0, 5, 10, 15 and 25%). The photo series exhibit a macroscopic shape-recovery process as indicated by arrows.

A typical procedure described here: the investigated samples with thickness of 0.15cm were tailoring into the letter shape of “iccas” as the permanent shape of the sample. Then all the letters were bent into a temporary helix shape at 80°C and the deformed shape is fixed at -20°C for 30min. When it is put in hot water of 80°C, it recovered to the original letter shape within 5 seconds. The photo series indicated by arrows were taken with a digital camera to record the shape recovery progress. It can be learnt from the macroscopic results that the pure PDLLA without HA component failed to recovery to its permanent shape, whereas the other tested groups were all performed well. The intuitive results demonstrated that the presence of HA nanoparticles played a key role in maintaining the permanent shape when shape deformation occurred, and thus reinforced the shape memory ability. However, it is hard to distinguish the differences of the shape memory abilities of the nanocomposites with various HA content by the macroanalysis alone.

To quantify the evaluation of shape-memory properties, cyclic thermo-mechanical test was performed.²¹ A well established four-step thermo mechanical cycling method (steps 1-4), which is also known as the “one-way shape memory (1WSM) cycle”,³⁹ was conducted by using a dynamic mechanical analyser (Q800 DMA, TA Instruments)

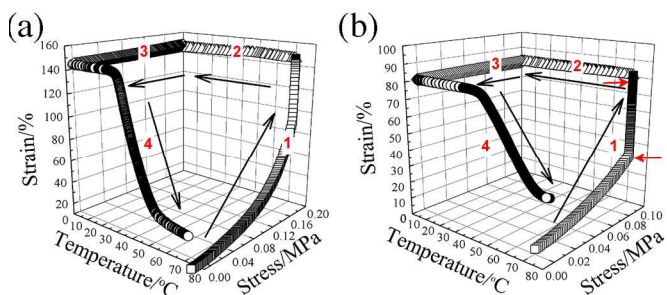


Fig 5. Stress-temperature-strain plots of one-way shape memory (1WSM) cycles of (a) HA15-g-PDLLA and (b) HA5-g-PDLLA.

As can be observed, in the case of HA15-g-PDLLA nanocomposites (Fig. 5a), a moderate strain of 145% was induced, the loading stress reached 0.2MPa in the initial stress-strain curve and the shape recovery ratio calculated according to the final strain-temperature curve is 81.8%. As a control, the SM cycle of HA5-g-PDLLA nanocomposites was investigated (Fig 5b). It was found that the stress-strain curve of HA5-g-PDLLA nanocomposites was nonlinear and the terminal of the curve has an abrupt shift. As indicated by the red arrows, the strain seems lost the control of the stress and immediately increased, where the large deformation occurred after yield point, resulting in a plastic, irreversible deformation because of

the slipping and disentangling of the polymer chains from each other.² Consequently, the plastic, irreversible deformation of HA5-g-PDLLA resulted in the poor SM recovery, the shape recovery ratio parameter (R_s) is only 58.5%. It is worth to point out that the pure PDLLA sample was so easy to produce large deformation that it failed to get the available SM cycle data.

To evaluate the lifetime of shape recovery cycles for the nanocomposites, more extensive cycling repeats were conducted for quantitative assessment. Figure 6 demonstrated four-step thermo mechanical cycling of the investigated samples repeating for three times. As shown in the Figure 6 a-d, when the samples deformed at 60°C and recovered at 60°C, the nanocomposites with different HA proportions show various SM behaviours.

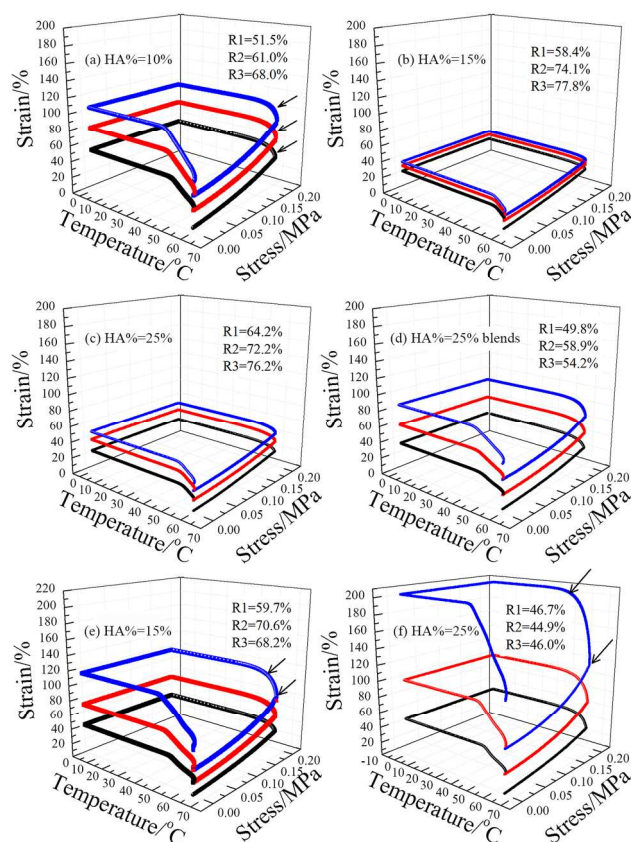


Fig 6. Three repeating cycle of stress-temperature-strain curves for different samples at 60°C (a-d) and 65°C (e&f).

The pure PDLLA had the poorest SM ability so that it failed to complete the three SM cycles. In the case of HA10-g-PDLLA nanocomposites, although the three repeating cycles were completed, the large damaging deformation process caused irreversible deformation. Especially it occurred during the second and third stress-strain curves, which caused the three circulate curves could not coincide completely. Consequently, the first strain percentage (strain₁) is 52.9%, while strain₂ is 81.2% and strain₃ reached up to 106.7%. The shape recovery ratio is 51.5%, 61% and 68%, correspondingly.

The HA15-g-PDLLA nanocomposites revealed the best cycle-repeating performance. As shown in the Fig 6b, the curves are much closer to coincidence, the strain₁ is 25.9%, while strain₂ is 32.6% and strain₃ is merely 37.4%. The corresponding shape recovery ratio is 58.4%, 74.1% and 77.8%.

Besides, it is worth to note that the HA25-g-PDLLA demonstrated better SM performances than HA/PDLLA blends. For the blends, due to the serious large deformation process caused by the weak interaction forces of hydrogen bonding between HA and PDLLA, the three repeating cycle curves were seriously diverged and the SM recovery ratio is 49.8%, 58.9% and 54.2%. On the contrast, the cycle curves of HA25-g-PDLLA are much closer and the SM recovery ratio is 64.2%, 72.2% and 76.2% correspondingly.

When the samples deformed at 65°C and recovered at 65°C (Fig. 6e&f), the large deformations were further aggravated. As for the HA15-g-PDLLA, the shape recovery ratio is 59.7%, 70.6% and 68.2% for the first, second and third SM repeating cycle, respectively. For HA25-g-PDLLA, the corresponding values were only 46.7%, 44.9% and 46.0%. The other samples, including pure PDLLA, HA5-g-PDLLA, HA10-g-PDLLA and HA25/PDLLA blends, failed to complete the three SM repeating cycles, attributing to the large damaging deformation process.

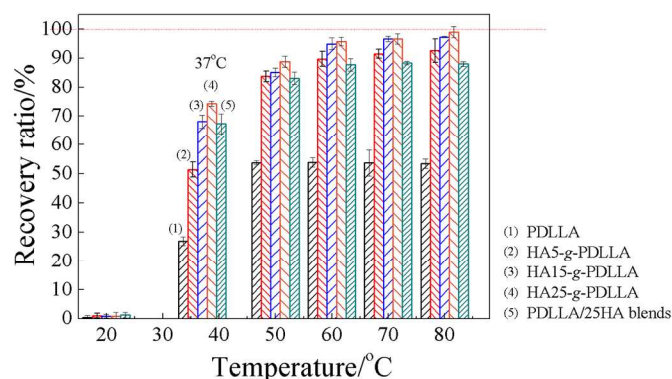


Fig 7. The effect of temperature on shape memory ratio of PDLLA and nanocomposites with different HA proportions.

In order to investigate the effect of temperature on the shape memory performances of nanocomposites, all the samples were evaluated at a temperature range of 20~80°C. Figure 7 demonstrated the plots of shape recovery ratio as a function of temperature. All the investigated samples (20×3×0.2mm) were incubated at 70°C for 10min and then elongated to L_d . Then the deformed samples were fixed by placing at -20°C for 30min. The shape memory performances at different temperature were observed. The shape memory ability of each sample was quantified by the shape recovery ratio parameter (R_r), defined by the following formula:

$$R_r = (L_d - L_f) / (L_d - L_0) \times 100\%$$

where L_0 represents original length, L_d is the length of deformed sample and L_f represents the final length of sample. It

can be learned from Figure 7 that the shape recovery ratio values were below 5% for all the investigated samples at 20°C, which means almost no recovery of the temporary shape can be observed. However, when all the deformed samples were placed at 37°C, which is close to the human physiological temperature, the R_r value reaches up to 68.1% for HA5-g-PDLLA and 74.3% for HA25-g-PDLLA. The excellent shape recovery performances were observed at 60°C, at which the R_r values reaches up to 89.7%, 94.9%, 95.7%, 87.7% for HA5-g-PDLLA, HA15-g-PDLLA, HA25-g-PDLLA nanocomposites and HA25/PDLLA blends respectively. When further heating up the samples up to 80°C, the shape recovery ratios approach to 100% for HA15-g-PDLLA and HA25-g-PDLLA. However, the pure PDLLA shows poor shape recovery ratio which is only 53.9% at 80°C.

It should be aware of the difference between the results obtained by manual experiments (Figure 7) and DMA analysis (Figure 6). As for Figure 7, the samples were transformed their shapes at certain temperature, and then directly put into refrigerator to fix their temporary shapes. After that, the samples were put in certain temperature environment again to recovery to the permanent shape. A series of procedures are quick and coherent. However, when the SM behaviours were conducted via DMA characterization, it required a constant speed to decrease and increase the temperature. It is found that the ‘relaxation process’ occurred during the course that the stress was removed and meanwhile the temperature still stayed above T_g . Because of the constant cooling rate, the shape transformation was still on going during this course. The shape deformation here was not under stress’s control, which was irreversible; it did not stop until the temperature decreased to certain value, the deformation was fixed finally. As a result, the shape memory behaviours of the nanocomposites conducted by DMA instrument demonstrated much worse than the manual experiments.

3.5 Mechanism of shape-memory effect for nanocomposites

The general mechanism of thermal-plastic SMPs has been discussed in many literatures.^{14,21,37,40} SMP exists in the form of polymer networks, in which the net points being connected by chain segments determine the permanent shape.¹ Typically, two components play a key role in the shape memory mechanism: one is “hard segments” acting as cross-linkers determining the permanent shape; and another is “soft segments” acting as continuous phase to fix the temporary shape at temperatures below transition temperature (T_{trans}).¹⁶ In the present case, amorphous polymer networks based on PDLLA matrixes took glass transition temperature as T_{trans} . While the grafted HA nanoparticles served as cross-linkers to sustain the skeleton of the inorganic-organic interpenetrated network. It has been well known that the cross-links can be either covalent bonds or physical interactions. On the basis of the above results, a mechanism model was supposed and illustrated in Figure 8.

The fixation of the HA in the PDLLA matrixes depending on the grafting chains intertwist with the free polymer chains. By this way, the HA nanoparticles were fixed in the polymer

network by covalent bonds interactions. As comparison, the shape fixity of amorphous PDLLA polymer depends on a random winding of molecular chains.²⁹ Consequently, the amorphous PDLLA performed poor shape recovery behaviour.

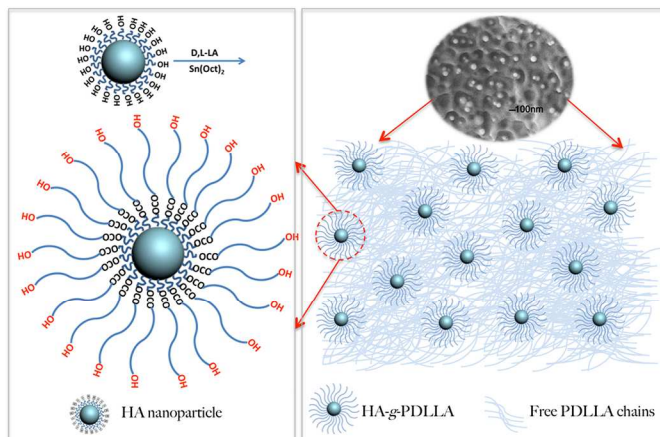


Fig 8. Schematic depiction of shape memory mechanism of HA-g-PDLLA nanocomposites.

According to the above investigations, the HA/PDLLA blends expressed an improved shape recovery ratio compared to the pure PDLLA polymer. The explanation to account for the phenomenon is lied on the physical crosslinking by connection of hydrogen bonding between HA and PDLLA.^{29,30} On basis of our investigations, the combining strength between the interfaces of organic and inorganic phases plays a key role in determining the shape memory ability of HA-g-PDLLA nanocomposites. It can be concluded that the SMPs deserve to the strong connection between the cross-links and the stationary phase to better memorize its permanent shape. Therefore, compared with the blends, the HA-g-PDLLA nanocomposites show more excellent shape memory performance.

3.6 Degradation and effect on shape memory properties of nanocomposites

As an excellent candidate for the minimally invasive surgery, the degradation of the scaffolds should be taken into consideration. In the present studies, HA-g-PDLLA was selected to be treated by alkaline solution to accelerate the degradation of PDLLA components. Our previous research showed an interesting phenomenon that the scaffold was covered with dense layer of HA nanoparticles after alkaline degradation.⁴¹ By means of this method, pre-degradation treatment on HA-g-PDLLA nanocomposites in this work was proceeded for two purposes: one is to obtain the biocompatible coating on the surfaces of the scaffolds, which make it potential in bone defect healing applications. Another is to reveal how the degradation affects the shape memory properties.

As illustrated in Figure 9, a dumbbell shaped HA15-g-PDLLA nanocomposites sheet with 65mm in length and 1.5mm in thickness was firstly immersed in alkaline solution (1M NaOH) for 1h. After then, the dried sample was deformed at 70°C. The sample was twisted twice and then quickly migrated to -20°C to

fix the temporary shape. When the sample was placed in 70°C atmosphere again, it recovered to the permanent shape in a rapid manner. Based on this phenomenon, the SM behaviour seemed not be affect by the degradation. SEM analysis confirmed that the surface of the sample was covered with intensive HA nanoparticles coating, as shown in Figure 9a.

Inspired by this interesting discovery, the weight loss as a function of degradation time and the corresponding shape recovery performance was further investigated. The HA15-g-PDLLA nanocomposites samples were first immersed in 1.0M alkaline solution for designed time (0.5h, 1h, 2h, 3h, 4h, 5h, 6h, 8h, 10h). After then, the samples were twisted twice at 70°C for shape deformation and stored at -20°C for shape fixation. Finally, the samples were placed at 70°C. The shapes of the samples before and after recovery were recorded by a digital camera. As shown in Figure 9b, even though the weight loss of HA15-g-PDLLA nanocomposite samples reach up to 65% after 10h degradation, and the samples appeared semi-transparent, they still successfully recovered to its permanent shape.

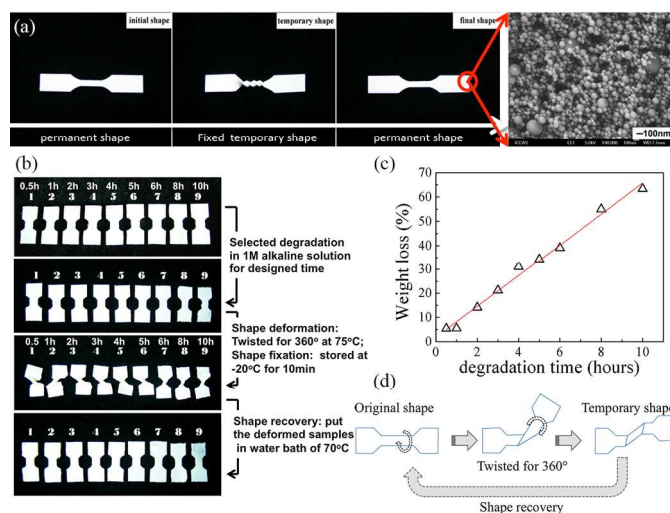


Fig 9. (a) & (b) Photographs of shape recovery process of alkaline-treated HA15-g-PDLLA; (c) Plots of weight loss as a function of degradation time; (d) Schematic pictures illustrated the shape recovery process.

If the nanocomposites were pre-degraded for overlong duration, it may affect the interfacial combination between two phases and thus cause damages to chemical networks of the nanocomposites, which not only affect the shape memory performance, but also deteriorate the functions of the polymers such as mechanical property. Therefore, appropriate alkaline pre-treatment is desirable to improve the biocompatibility and biomimetic mineralization *in vitro* while not to deteriorate the shape memory properties of the materials.

4. Conclusions

Biodegradable polymer-based nanocomposites with excellent shape-memory properties were developed. The HA-g-PDLLA nanocomposites with various HA proportions were synthesized via *in-situ* grafting polymerization. With the incorporation of HA nanoparticles, the nanocomposites possess desirable shape

memory abilities, which was satisfied with macroscopic applications. The excellent shape memory properties were observed from nanocomposites with 15% weight fraction of HA contents. The HA25-g-PDLLA nanocomposites and HA25/PDLLA blends were compared, and the former showed the better shape memory property due to the *in-situ* grafting polymerization. The mechanism investigation suggested that the uniformly dispersed grafting HA nanoparticles were fixed in the polymer network by covalent bonds interactions, make HA functioned as hard segments to prevent the mobility of the PDLLA chains. The intensive HA nanoparticles coating on HA-g-PDLLA nanocomposites resulted from appropriate alkaline-treatment did not deteriorate shape memory property, but showed great potentials in biomedical application.

5. Acknowledgements

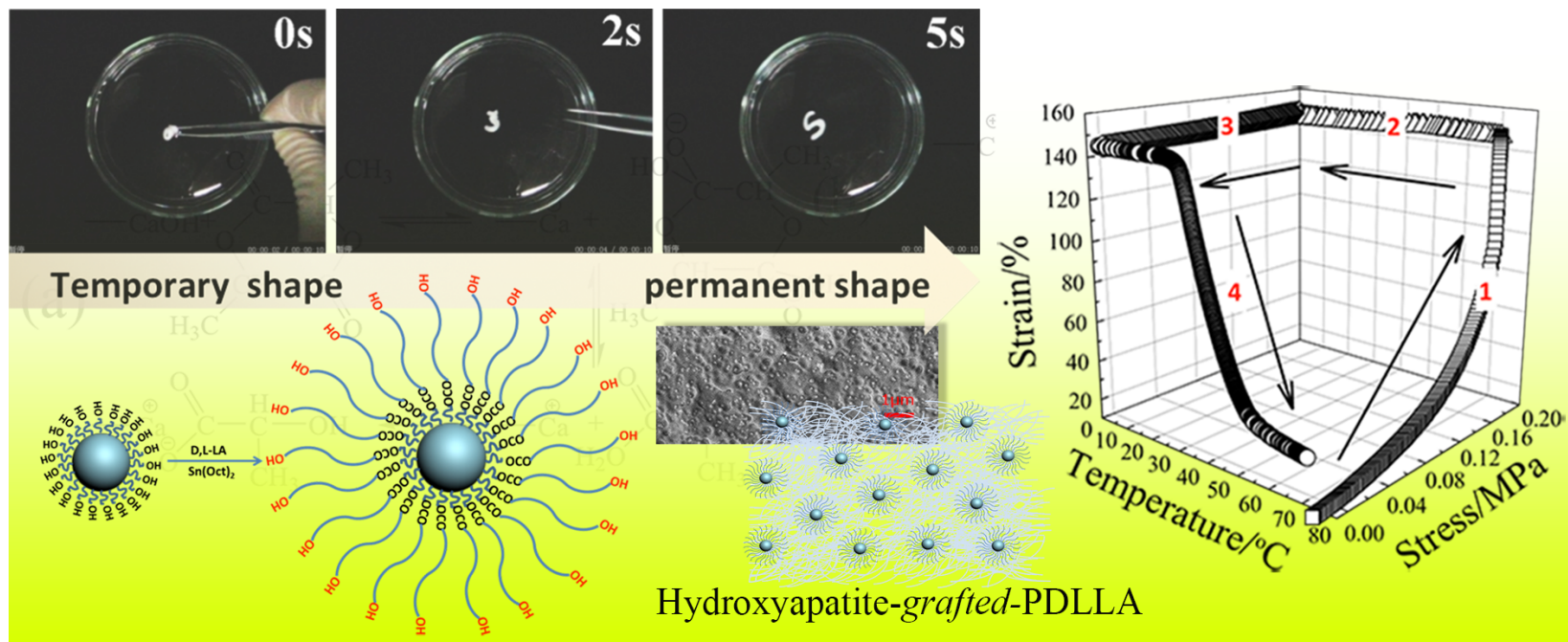
This work is supported by the Natural Science Foundation of China (Grant No. 51025314) and the "Strategic Priority Research Program" of the Chinese Academy of Sciences (Grant No. XDA01030301).

6. Notes and references

^a The CAS Key Laboratory of Engineering Plastics, Institute of Chemistry, Chinese Academy of Sciences (CAS), Beijing 100190, China

^b The State Key Laboratory of Organic-Inorganic Composites, Beijing Laboratory of Biomedical Materials, College of Life Science and Technology, Beijing University of Chemical Technology, Beijing 100029, China

1. M. Behl, M. Y. Razzaq and A. Lendlein, *Advanced Materials*, 2010, **22**, 3388-3410.
2. A. Lendlein and S. Kelch, *Angew. Chem. Int. Ed.*, 2002, **41**, 2034 - 2057.
3. P. Miaudet, A. Derre, M. Maugey, C. Zakri, P. M. Piccione, R. Inoubli and P. Poulin, *Science*, 2007, **318**, 1294-1296.
4. J. F. Mano, *Advanced Engineering Materials*, 2008, **10**, 515-527.
5. A. Lendlein, H. Y. Jiang, O. Junger and R. Langer, *Nature*, 2005, **434**, 879-882.
6. T. Miyata, N. Asami and T. Urugami, *Nature*, 1999, **399**, 766-769.
7. R. Mohr, K. Kratz, T. Weigel, M. Lucka-Gabor, M. Moneke and A. Lendlein, *Proceedings of the National Academy of Sciences of the United States of America*, 2006, **103**, 3540-3545.
8. S. J. Kim, H. I. I. Kim, S. J. Park and S. I. Kim, *Sens. Actuator A-Phys.*, 2004, **115**, 146-150.
9. G. Rabani, H. Luftmann and A. Kraft, *Polymer*, 2006, **47**, 4251-4260.
10. T. Chung, A. Rorno-Urbe and P. T. Mather, *Macromolecules*, 2008, **41**, 184-192.
11. A. Lendlein, J. Zotzmann, Y. K. Feng, A. Alteheld and S. Kelch, *Biomacromolecules*, 2009, **10**, 975-982.
12. I. A. Rousseau, *Polymer Engineering & Science*, 2008, **48**, 2075-2089.
13. J. Li and T. Xie, M, *Macromolecules* 2011, **44**, 175-180.
14. M. Behl and A. Lendlein, *Materials Today*, 2007, **10**, 20-28.
15. Y. S. Wong and S. S. Venkatraman, *Acta Materialia*, 2010, **58**, 49-58.
16. A. Alteheld, Y. K. Feng, S. Kelch and A. Lendlein, *Angewandte Chemie-International Edition*, 2005, **44**, 1188-1192.
17. B.C. Guo, Y.W. Chen, Y.D. Lei, L.Q. Zhang, W.Y. Zhou, A.B.M Rabie, and J.Q. Zhao, *Biomacromolecules* 2011, **12**, 1312-1321.
18. C. Wischke, A. T. Neffe, S. Steuer and A. Lendlein, *Journal of controlled release: official journal of the Controlled Release Society*, 2009, **138**, 243-250.
19. M. C. Chen, Y. Chang, C. T. Liu, W. Y. Lai, S. F. Peng, Y. W. Hung, H. W. Tsai and H. W. Sung, *Biomaterials*, 2009, **30**, 79-88.
20. A. Lendlein and R. Langer, *Science*, 2002, **296**, 1673-1676.
21. W. Small, T. S. Wilson, W. J. Benett, J. M. Loge and D. J. Maitland, *Optics Express*, 2005, **13**, 8204-8213.
22. G. Lim, K. Park, M. Sugihara, K. Minami and M. Esashi, *Sensors and Actuators a-Physical*, 1996, **56**, 113-121.
23. A. J. Thornton, E. Alsberg, M. Albertelli and D. J. Mooney, *Transplantation*, 2004, **77**, 1798-1803.
24. K. Nagahama, Y. Ueda, T. Ouchi, Y. Ohya, *Biomacromolecules*, 2009, **10**, 1789-1794.
25. E. Zini, M. Scandola, P. Dobrzynski, J. Kasperczyk and M. Bero, *Biomacromolecules*, 2007, **8**, 3661-3667.
26. M. Lebourg, J. S. Anton and J. L. G. Ribelles, *Journal of Materials Science-Materials in Medicine*, 2010, **21**, 33-44.
27. E. Nejati, H. Mirzadeh and M. Zandi, *Composites Part a-Applied Science and Manufacturing*, 2008, **39**, 1589-1596.
28. C. L. Yang, K. Cheng, W. J. Weng and C. Y. Yang, *Journal of Materials Science-Materials in Medicine*, 2009, **20**, 667-672.
29. S. B. Zhou, X. T. Zheng, X. J. Yu, J. X. Wang, J. Weng, X. H. Li, B. Feng and M. Yin, *Chemistry of Materials*, 2007, **19**, 247-253.
30. X. T. Zheng, S. B. Zhou, X. H. Li and H. Weng, *Biomaterials*, 2006, **27**, 4288-4295.
31. E. Helwig, B. Sandner, U. Gopp, F. Vogt, S. Wartewig and S. Henning, *Biomaterials*, 2001, **22**, 2695-2702.
32. K. Chrissafis, G. Antoniadis, K. M. Paraskevopoulos, A. Vassiliou and D. N. Bikiaris, *Composites Science and Technology*, 2007, **67**, 2165-2174.
33. L. Q. Liao, C. Zhang and S. Q. Gong, *Macromolecular Rapid Communications*, 2007, **28**, 1148-1154.
34. H. J. Lee, H. W. Choi, K. J. Kim and S. C. Lee, *Chemistry of Materials*, 2006, **18**, 5111-5118.
35. Z. K. Hong, X. Y. Qiu, J. R. Sun, M. X. Deng, X. S. Chen and X. B. Jing, *Polymer*, 2004, **45**, 6699-6706.
36. S. C. Lee, H. W. Choi, H. J. Lee, K. J. Kim, J. H. Chang, S. Y. Kim, J. Choi, K. S. Oh and Y. K. Jeong, *Journal of Materials Chemistry*, 2007, **17**, 174-180.
37. Y. P. Liu, K. Gall, M. L. Dunn, P. McCluskey, *Mechanics of Materials* 2004, **36**, 929-940.
38. X. Zheng, S. B. Zhou, Y. Xiao, X. J. Yu, X. H. Li, P. Z. Wu, *Colloids and Surfaces B-Biointerfaces* 2009, **71**, 67-72.
39. P. T. Knight, K. M. Lee, T. Chung, P. T. Mather, *Macromolecules* 2009, **42**, 6596-6605.
40. H. Zhang, H. Wang, W. Zhong, Q. Du, *Polymer* 2009, **50**, 1596-1601.
41. K. Du, X. Shi and Z. Gan, *Langmuir* 2013, **29**, 15293-15301.



The HA nanoparticles grafted in PDLLA matrix play an important role for HA-g-PDLLA nanocomposites with excellent shape memory property.